REPORT 1147

THE SIMILARITY LAW FOR HYPERSONIC FLOW AND REQUIREMENTS FOR DYNAMIC SIMILARITY OF RELATED BODIES IN FREE FLIGHT [1]

By Frank M. Hamaker, Stanford E. Neice, and Thomas J. Wong

SUMMARY

The similarity law for nonsteady, inviscid, hypersonic flow about slender three-dimensional shapes is derived in terms of customary aerodynamic parameters. The conclusions drawn from the potential analysis used in the development of the law are shown to be valid for rotational flow. A direct consequence of the hypersonic similarity law is that the ratio of the local static pressure to the free-stream static pressure is the same at corresponding points in similar flow fields.

Requirements for dynamic similarity of related shapes in free flight, including the correlation of their flight paths, are obtained using the aerodynamic forces and moments as correlated by the hypersonic similarity law. In addition to the conditions of hypersonic similarity, dynamic similarity depends upon conditions derived from the inertial properties of the bodies and the immersing fluids. In order to have dynamic similarity, however, rolling motions must not occur in combination with other motions.

The law is examined for steady flow about related three-dimensional shapes. The results of a computational investigation showed that the similarity law as applied to nonlifting cones and ogives is applicable over a wide range of Mach numbers and fineness ratios. In the special case of inclined bodies of revolution, the law is extended to include some significant effects of the viscous cross force. Results of a limited experimental investigation of the pressures acting on two inclined cones are found to check the law as it applies to bodies of revolution.

INTRODUCTION

The hypersonic similarity law for steady potential flows about thin airfoil sections and slender nonlifting bodies of revolution was first developed by Tsien in reference 1. Hayes (ref. 2) investigated this law from the standpoint of analogous nonsteady flows and concluded that it would also apply to nonpotential flows containing shock waves and vorticity, provided the local Mach number was everywhere large with respect to 1. He also reasoned that similitude could be obtained in hypersonic flows about slender three-dimensional bodies of arbitrary shape; however, the form of the similarity law in terms of customary aerodynamic parameters was not determined. Oswatitsch (ref. 3) investigated the law for two-dimensional steady flow in the limiting case where the Mach number tends toward infinity and, hence, ceases to be a flow parameter. His formulation of the law, therefore, involves only thickness ratio and angle of attack. Goldsworthy (ref. 4) investigated the effects of rotation on the hypersonic similarity law for two-dimensional steady flow. His results corroborated, in part, the previous findings of Hayes and showed the potential analysis of Tsien to be valid.

An investigation of the law as it applies in nonsteady flow was made by Lin, Reissner, and Tsien (ref. 5). In particular, the necessary conditions for similarity of hypersonic flow about oscillating two-dimensional bodies were determined. The analysis for more arbitrary motion of two- or three-dimensional bodies is apparently not available.

Ehret, Rossow, and Stevens (ref. 6) investigated the hypersonic similarity law for steady flow about nonlifting bodies of revolution by comparing pressure distributions calculated by means of the method of characteristics. They found the law to be applicable over a wide range of Mach numbers and thickness ratios. Their investigation did not, however, include the effects of vorticity arising from the curvature of the nose shock wave. Rossow (ref. 7) continued this investigation and found that the law was equally valid when the effects of vorticity were included in the calculations. These findings corroborated, in part, the observations of Hayes and indicated that the law may be used with confidence to investigate the aerodynamic characteristics for steady flow about nonlifting bodies of revolution at hypersonic speeds.

It appears desirable, therefore, to attempt to unify the different treatments of the similarity law into a single formulation. The primary purpose of this report is, then, to determine the form of the hypersonic similarity law for nonsteady flow about slender three-dimensional bodies of arbitrary shape and to present the results in terms of customary aerodynamic parameters. It is further undertaken to examine the hypersonic similarity law in some detail as it applies to steady flow.

The possibility of obtaining a hypersonic similarity law for correlating the aerodynamic forces and moments on related shapes in free flight suggests a more general dynamic problem, that of correlating their motions with the aid of this law. Hence, it is also undertaken in this report to determine the requirements on the inertial properties of related bodies and the immersing fluids in order that such bodies may have similar free-flight paths, that is, dynamic similarity.

[1] Supersedes NACA TN 2443, "The Similarity Law for Hypersonic Flow About Slender Three-Dimensional Shapes," by Frank M. Hamaker, Stanford E. Neice, and A. J. Eggers, Jr., 1951, and NACA TN 2631, "The Similarity Law for Nonsteady Hypersonic Flows and Requirements for the Dynamical Similarity of Related Bodies in Free Flight," by Frank M. Hamaker and Thomas J. Wong, 1952.

SYMBOLS

a	speed of sound
A	characteristic reference area of body, $A=bt$
b	characteristic width of body
C_C	side-force coefficient, $\frac{\text{side force}}{\frac{1}{2}\rho_0 V_0^2 A}$
$\tilde{C}_C$	side-force function
C_D	drag coefficient, $\frac{\text{drag}}{\frac{1}{2}\rho_0 V_0^2 A}$
$\tilde{C}_D$	drag function
C_l	rolling-moment coefficient, $\frac{\text{rolling moment}}{\frac{1}{2}\rho_0 V_0^2 A b}$
$\tilde{C}_l$	rolling-moment function
C_L	lift coefficient, $\frac{\text{lift}}{\frac{1}{2}\rho_0 V_0^2 A}$
$\tilde{C}_L$	lift function
C_m	pitching-moment coefficient, $\frac{\text{pitching moment}}{\frac{1}{2}\rho_0 V_0^2 A c}$
$\tilde{C}_m$	pitching-moment function
C_n	yawing-moment coefficient, $\frac{\text{yawing moment}}{\frac{1}{2}\rho_0 V_0^2 A b}$
$\tilde{C}_n$	yawing-moment function
C_p	specific heat at constant pressure
C_v	specific heat at constant volume
c	characteristic length of body
c_{d_c}	section drag coefficient of circular cylinder with axis perpendicular to the flow
$\hat{c}_{d_c}$	mean c_{d_c} for a body of revolution
D	displaced-fluid-mass factor, $\frac{cbt\rho_0}{2}$
d	length of flight path
F	viscous force or moment function
f	dimensionless perturbation potential function
fn	general functional designation
G	body-shape function
g	dimensionless body-shape function
$\bar{h}$	vector from the origin of the coordinate system to any point on the body
$\bar{i},\bar{j},\bar{k}$	unit vectors along coordinate axes x,y,z, respectively
I_{x-x}, I_{y-y}, I_{z-z}	moments of inertia of body about the x,y,z axes, respectively
$K_t=M_0\frac{t}{c}$, $K_b=M_0\frac{b}{c}$; $K_\alpha=M_0\alpha$, $K_\beta=M_0\beta$; $K_\delta=\delta$, $K_p=M_0\left(\frac{pb}{V_0}\right)$; $K_q=M_0\left(\frac{qc}{V_0}\right)$, $K_r=M_0\left(\frac{rc}{V_0}\right)$	hypersonic similarity parameters
$K_{x-x}=\frac{c^2D}{I_{x-x}}$, $K'_{x-x}=\frac{b^2D}{I_{x-x}}$, $K_{y-y}=\frac{c^2D}{I_{y-y}}$; $K_{z-z}=\frac{c^2D}{I_{z-z}}$, $K_\mu=\frac{D}{\mu}$	dynamic similarity parameters
l,m,n	direction cosines of the unit outer normal vector to the body surface
M	Mach number
M_x,M_y,M_z	moments acting on body about x,y,z axes, respectively
$\bar{N}$	unit outer normal vector to surface of body
P	static pressure
p,q,r	rolling, pitching, and yawing velocities, respectively
R	radius of curvature of flight path
R_c	cross Reynolds number based on maximum body diameter and the component of the free-stream velocity normal to the body axis
r	radius of body of revolution at any station x
s	cross force per unit length
t	characteristic depth of body
u,v,w	components of body velocity along the x,y,z axes, respectively
V	resultant velocity
x,y,z	Cartesian coordinates fixed relative to the body
X,Y,Z	forces on body along x,y,z axes, respectively
α	angle of attack
β	angle of sideslip
γ	ratio of the specific heats, $\gamma=\frac{C_p}{C_v}$
δ	angle of roll
ϵ	orifice location on the test cones
ξ,η,ζ	dimensionless coordinates corresponding to x,y,z, respectively
θ	time coordinate
μ	mass of body
ρ	density of the fluid
τ	dimensionless time coordinate, $\frac{a_0 M_0 \theta}{c}$
φ	perturbation potential function
Φ	potential function
ψ,Ω	alternate time variables
ω	angular velocity of the body

SUBSCRIPTS

0	free-stream conditions
v	viscous cross-force effects
1,2,3	different functions F, C_m, or C_n, except as noted

SUPERSCRIPT

$-$	vector quantities

Except for symbols noted above, all variables used as subscripts indicate partial differentiation with respect to the subscript variable.

THE SIMILARITY LAW FOR NONSTEADY THREE-DIMENSIONAL FLOW

DEVELOPMENT OF THE LAW

The hypersonic similarity law is derived from the equations of motion and energy and from the boundary conditions. In deriving the law, the following assumptions are made: (1) The Mach number of the uniform stream is large compared to 1; (2) the disturbance velocities are small compared

to the free-stream velocities; and (3) the flow is of the potential type. These assumptions imply that the analysis is restricted to hypersonic flow over slender bodies at small angles of attack and to irrotational flows, respectively. As was indicated in the introduction, the law has been extended to rotational flows by both Hayes and Goldsworthy. An analysis is presented in Appendix A to show that the rotational effects in a three-dimensional nonsteady flow obey the hypersonic similarity law as formulated by the potential analysis. Hence, the conclusions derived from the analysis based upon potential flow will also be valid for rotational flow. The purpose of making the assumption of potential flow is merely to simplify the analysis.

The coordinate system is fixed with respect to the body, as shown in figure 1. Also shown are the possible angular velocities of the body and the direction of the velocity vector of the free stream. The angles have the conventional positive sense of angles of attack and sideslip. Under assumption (2), these angles must be small.

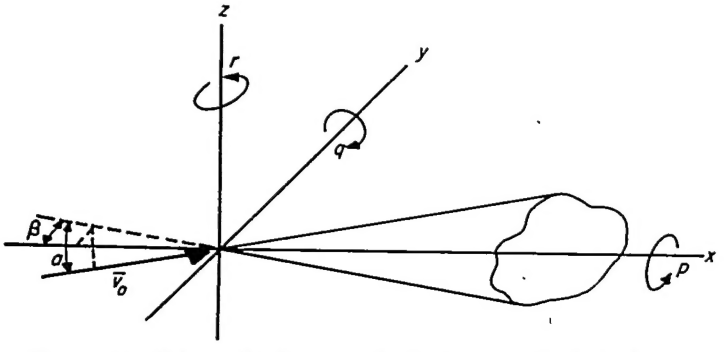

FIGURE 1.—Schematic diagram of orientation of body in flow.

The development of the law involves, first, derivation of a simplified potential equation describing the flow, second, the statement of the boundary conditions, and third, the transformation of these equations into nondimensional coordinates.

The simplified potential equation is obtained from the nonsteady equation of motion and the energy equation which are written in the following potential form:

$$\Phi_{\theta\theta}+\Phi_{xx}(\Phi_x^2-a^2)+\Phi_{yy}(\Phi_y^2-a^2)+\Phi_{zz}(\Phi_z^2-a^2)+$$
$$2(\Phi_{xy}\Phi_x\Phi_y+\Phi_{yz}\Phi_y\Phi_z+\Phi_{xz}\Phi_x\Phi_z)+$$
$$2(\Phi_x\Phi_{x\theta}+\Phi_y\Phi_{y\theta}+\Phi_z\Phi_{z\theta})=0 \tag{1a}$$

$$\Phi_\theta+\frac{1}{2}(\Phi_x^2+\Phi_y^2+\Phi_z^2)+\frac{a^2}{\gamma-1}=\frac{V_0^2}{2}+\frac{a_0^2}{\gamma-1} \tag{1b}$$

These equations are expanded by expressing the potential-function derivatives in the following perturbation form:

$$\left.\begin{aligned}\Phi_x&=V_0-\frac{V_0\alpha^2}{2}-\frac{V_0\beta^2}{2}+\varphi_x\\ \Phi_y&=-V_0\beta+\varphi_y\\ \Phi_z&=V_0\alpha+\varphi_z\\ \Phi_\theta&=\varphi_\theta\end{aligned}\right\} \tag{2}$$

The local speed of sound a can be eliminated by combining the expanded forms of equations (1b) and (1a). The resulting equation can be simplified by neglecting higher order terms keeping in mind that for hypersonic flows about slender shapes φ_x, φ_y, φ_z, and a_0 are small compared to V_0 and that φ_x is small compared to φ_y and φ_z. The simplified potential equation then assumes the following form:

$$\frac{\varphi_{\theta\theta}}{a_0^2}+M_0^2\varphi_{xx}+\varphi_{yy}\left[M_0^2\beta^2+(\gamma-1)\frac{M_0}{a_0}\varphi_x-(\gamma+1)\frac{M_0}{a_0}\beta\varphi_y+\right.$$
$$\left.(\gamma-1)\frac{M_0}{a_0}\alpha\varphi_z+\frac{\gamma+1}{2}\frac{\varphi_y^2}{a_0^2}+\frac{\gamma-1}{2}\frac{\varphi_z^2}{a_0^2}+(\gamma-1)\frac{\varphi_\theta}{a_0^2}-1\right]+$$
$$\varphi_{zz}\left[M_0^2\alpha^2+(\gamma-1)\frac{M_0}{a_0}\varphi_x-(\gamma-1)\frac{M_0}{a_0}\beta\varphi_y+(\gamma+1)\frac{M_0}{a_0}\alpha\varphi_z+\right.$$
$$\left.\frac{\gamma-1}{2}\frac{\varphi_y^2}{a_0^2}+\frac{\gamma+1}{2}\frac{\varphi_z^2}{a_0^2}+(\gamma-1)\frac{\varphi_\theta}{a_0^2}-1\right]+2\left[M_0\varphi_{xy}\left(-M_0\beta+\frac{\varphi_y}{a_0}\right)+\right.$$
$$\varphi_{yz}\left(-M_0^2\alpha\beta-\frac{M_0\beta\varphi_z}{a_0}+\frac{M_0\alpha\varphi_y}{a_0}+\frac{\varphi_y\varphi_z}{a_0^2}\right)+M_0\varphi_{xz}\left(-M_0\alpha+\right.$$
$$\left.\left.\frac{\varphi_z}{a_0}\right)\right]+2\left(\frac{M_0\varphi_{x\theta}}{a_0}-\frac{M_0\beta\varphi_{y\theta}}{a_0}+\frac{\varphi_y\varphi_{y\theta}}{a_0^2}+\frac{M_0\alpha\varphi_{x\theta}}{a_0}+\frac{\varphi_z\varphi_{z\theta}}{a_0^2}\right)=0 \tag{3}$$

The shape of the body can be expressed by the functional relation

$$G(x,y,z)=0 \tag{4}$$

The unit outer normal at a point on the body surface is given by the vector

$$\vec{N}=l\vec{i}+m\vec{j}+n\vec{k} \tag{5}$$

and the requirement that the body be slender is satisfied by the condition

$$l<<1 \tag{6}$$

There are two boundary conditions which must be satisfied. The first of these is that the perturbation velocity, imposed by the presence of the body, must vanish at large distances ahead of the body. Consequently,

$$\varphi_x=\varphi_y=\varphi_z=0 \text{ at } x=-\infty \tag{7}$$

The other boundary condition is given by the fact that the flow is tangent to the body at the surface, that is, for no angular velocity

$$\vec{N}\cdot\vec{V}=0 \tag{8}$$

The angular velocity of a body will cause an apparent distortion of the velocity vector at the surface of the body. By expressing the angular velocity in the form,

$$\vec{\omega}=p\vec{i}+q\vec{j}+r\vec{k} \tag{9}$$

the velocity of each point on the surface of the body is then given by the vector cross product

$$\vec{\omega}\times\vec{h}=(qz-ry)\vec{i}+(rx-pz)j+(py-qx)\vec{k} \tag{10}$$

The boundary condition on the surface of the body then becomes

$$(\vec{V}-\vec{\omega}\times\vec{h})\cdot\vec{N}=0 \tag{11}$$

After equation (10) is expanded and combined with equation (11), and higher order terms neglected in accordance with equation (6), the second boundary condition assumes the following form:

$$V_0G_x-(V_0\beta-\varphi_y+rx-pz)G_y+(V_0\alpha+\varphi_z+qx-py)G_z=0 \text{ at } G=0 \tag{12}$$

In obtaining the similarity law for flow about related bodies, the equations of motion and boundary conditions are expressed in a nondimensional form. A nondimensional coordinate system is introduced by the following affine transformation:

$$\xi=\frac{x}{c},\ \eta=\frac{y}{b},\ \zeta=\frac{z}{t},\ \tau=\frac{\theta a_0 M_0}{c} \tag{13}$$

and a nondimensional perturbation potential function is defined by the relation

$$f(\xi,\eta,\zeta,\tau)=\frac{\varphi(x,y,z,\theta)}{a_0M_0c\left(\frac{t}{c}\right)^2} \tag{14}$$

where c, b, and t are a characteristic length, width, and depth of the body, respectively. Under the coordinate transformation given above, equation (4) takes the form

$$g(\xi,\eta,\zeta)=0 \tag{15}$$

By substitution of equations (13) and (14), equations (3), (7), and (12) become, respectively,

$$K_t^2(f_{\tau\tau}+f_{\xi\xi})+\left(\frac{K_t}{K_b}\right)^2 f_{\eta\eta}\left[K_\beta^2+(\gamma-1)K_t^2f_\xi-(\gamma+1)\left(\frac{K_t}{K_b}\right)K_tK_\beta f_\eta+(\gamma-1)K_tK_\alpha f_\zeta+\frac{\gamma+1}{2}\left(\frac{K_t}{K_b}\right)^2K_t^2f_\eta^2+\frac{\gamma-1}{2}K_t^2f_\zeta^2+(\gamma-1)K_t^2f_\tau-1\right]+f_{\zeta\zeta}\left[K_\alpha^2+(\gamma-1)K_t^2f_\xi-(\gamma-1)\left(\frac{K_t}{K_b}\right)K_tK_\beta f_\eta+(\gamma+1)K_tK_\alpha f_\zeta+\frac{\gamma-1}{2}\left(\frac{K_t}{K_b}\right)^2K_t^2f_\eta^2+\frac{\gamma+1}{2}K_t^2f_\zeta^2+(\gamma-1)K_t^2f_\tau-1\right]+2\left\{\left(\frac{K_t}{K_b}\right)f_{\xi\eta}\left[\left(\frac{K_t}{K_b}\right)K_t^2f_\eta-K_tK_\beta\right]+\left(\frac{K_t}{K_b}\right)f_{\eta\zeta}\left[-K_\alpha K_\beta-K_tK_\beta f_\zeta+K_t\left(\frac{K_t}{K_b}\right)f_\eta(K_\alpha+K_tf_\zeta)\right]+K_tf_{\zeta\xi}(K_\alpha+K_tf_\zeta)\right\}+2\left\{K_t^2f_{\xi\tau}-\left(\frac{K_t}{K_b}\right)f_{\eta\tau}\left[K_tK_\beta+\left(\frac{K_t}{K_b}\right)K_t^2f_\eta\right]+K_tf_{\zeta\tau}(K_\alpha+K_tf_\zeta)\right\}=0 \tag{16}$$

$$f_\tau=f_\xi=f_\eta=f_\zeta=0 \quad \text{at} \quad \xi=-\infty \tag{17}$$

$$g_\xi-\left[\left(\frac{K_\beta}{K_b}\right)-\left(\frac{K_t}{K_b}\right)^2f_\eta+\left(\frac{K_\tau}{K_b}\right)\xi-\frac{K_p}{K_t}\left(\frac{K_t}{K_b}\right)^2\zeta\right]g_\eta+\left[\left(\frac{K_\alpha}{K_t}\right)+f_\zeta+\left(\frac{K_q}{K_t}\right)\xi-\left(\frac{K_p}{K_t}\right)\eta\right]g_\zeta=0 \tag{18}$$

where

$$K_t=M_0\frac{t}{c} \tag{19}$$

$$K_b=M_0\frac{b}{c} \tag{20}$$

$$K_\alpha=M_0\,\alpha \tag{21}$$

$$K_\beta=M_0\,\beta \tag{22}$$

$$K_p=M_0\left(\frac{pb}{V_0}\right) \tag{23}$$

$$K_q=M_0\left(\frac{qc}{V_0}\right) \tag{24}$$

$$K_r=M_0\left(\frac{rc}{V_0}\right) \tag{25}$$

It is seen then that, if two related bodies are flying with given motions and attitudes so that the parameters, equations (19) through (25), are the same for both bodies, the flows are characterized by the same function $f(\xi,\eta,\zeta,\tau)$ and are therefore similar. The requirements expressed by the nondimensional form of the body-shape function, equation (15), and the similarity parameters, equations (19) through (25), therefore constitute the similarity law of hypersonic flow.

A closer examination of the parameters K_t, K_b, K_α, and K_β reveals that an essential property of similarity is that the lateral dimensions and the slopes of a body with respect to the flow direction are in inverse proportion to the flight Mach number. In fact, the remaining parameters K_p, K_q, and K_r, which relate to nonsteady motion of the body, can be interpreted by means of the same property. In rolling, for example, points on the body surface perform helical motions, and the quantity pb/V_0 in equation (23) is simply proportional to the slope of the helix with respect to the flow direction. This slope must be inversely proportional to the flight Mach number. Similar arguments may be applied to K_q and K_r.

Because of the complexities of algebra involved, the effects of angle of roll were not included in the previous equations. Had they been included, however, the result would be the same as above with the additional requirement that the angle of roll must be the same for the related bodies. Hence, the additional hypersonic similarity parameter is

$$K_\delta=\delta \tag{26}$$

CORRELATION OF AERODYNAMIC FORCES AND MOMENTS

The correlation of aerodynamic forces and moments on related bodies in unsteady hypersonic flows can be developed by consideration of the pressure distribution over the bodies. The pressure relation is obtained from the energy equation, equation (2), and is given in the following form:

$$\frac{P}{P_0}=\left[\frac{1+\frac{\gamma-1}{2a_0^2}V_0^2}{1+\frac{\gamma-1}{2a^2}(V^2+2\phi_\theta)}\right]^{\frac{\gamma}{\gamma-1}} \tag{27}$$

When this expression is simplified (in a manner paralleling the development of the preceding section) to include only higher order terms and put into nondimensional form, it

reduces to a function only of the nondimensional coordinates and the similarity parameters (for a constant γ).

$$\frac{P}{P_0}=\frac{P}{P_0}(\xi, \eta, \zeta, \tau; K_t, K_b, K_\alpha, K_\beta, K_\delta, K_p, K_q, K_r) \quad (28)$$

It is clear from this relation that for similar flows, the ratio of the local to the free-stream static pressure is the same at corresponding points in the flow fields.[2]

The correlation of the aerodynamic forces and moments is then obtained with the aid of equation (28) by integration of the appropriate components of the pressure forces over the related shapes. This correlation can be given in the following forms:

$$\left.\begin{aligned} M_0C_L&=\tilde{C}_L=\tilde{C}_L(K_t, K_b, K_\alpha, K_\beta, K_\delta, K_p, K_q, K_r)\\ M_0^2C_D&=\tilde{C}_D=\tilde{C}_D(K_t, K_b, K_\alpha, K_\beta, K_\delta, K_p, K_q, K_r)\\ M_0C_C&=\tilde{C}_C=\tilde{C}_C(K_t, K_b, K_\alpha, K_\beta, K_\delta, K_p, K_q, K_r)\\ M_0C_m&=\tilde{C}_m=\tilde{C}_{m_1}(K_t \ldots K_r)+\frac{1}{M_0^2}\tilde{C}_{m_2}(K_t \ldots K_r)\\ C_n&=\tilde{C}_n=\tilde{C}_{n_1}(K_t \ldots K_r)+\frac{1}{M_0^2}\tilde{C}_{n_2}(K_t \ldots K_r)\\ M_0C_l&=\tilde{C}_l=\tilde{C}_l(K_t \ldots K_r) \end{aligned}\right\} \quad (29)$$

It appears, from the equations for the pitching-moment and yawing-moment functions of equation (29), that these two functions cannot be correlated for related but otherwise arbitrary body shapes. However, a careful examination of the order of magnitude involved in the analysis indicates that the second term on the right in these expressions becomes negligible in magnitude in all but two very special cases. In the case of the pitching-moment function, both terms on the right side become of the same order of magnitude when the l and n components of the unit normal to the body surface are very small. This condition corresponds to an isolated vertical fin as shown in figure 2 (a). If, however, the vertical fin is mounted on a body, or used in combination with a body equipped with horizontal wings, the contribution of the vertical fin to the total pitching moment will be very small indeed. The contribution of the second term in the pitching-moment function for the entire body will, of course, be correspondingly small. An analogous situation exists in the yawing-moment function for an isolated wing (fig. 2 (b)) in which the l and m components of the unit normal vector are both small. For most practical aerodynamic shapes, therefore, the offending terms can be neglected, and correlation of the aerodynamic coefficients can be achieved as shown in the following relations:

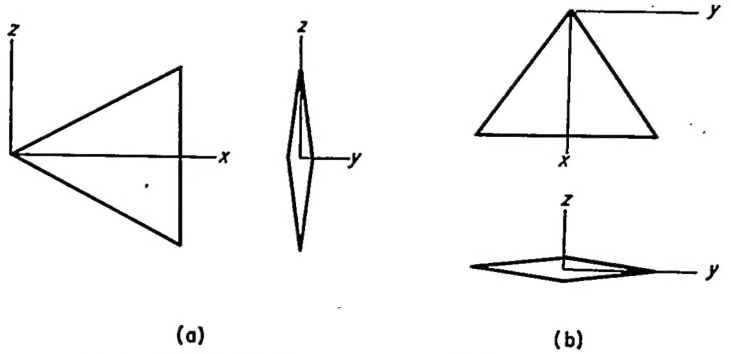

(a) (b)

(a) Pitching moment. (b) Yawing moment.

FIGURE 2.—Bodies excluded from similarity considerations as applied to pitching and yawing moments.

$$\left.\begin{aligned} M_0C_L&=\tilde{C}_L=\tilde{C}_L(K_t, K_b, K_\alpha, K_\beta, K_\delta, K_p, K_q, K_r)\\ M_0^2C_D&=\tilde{C}_D=\tilde{C}_D(K_t, K_b, K_\alpha, K_\beta, K_\delta, K_p, K_q, K_r)\\ M_0C_C&=\tilde{C}_C=\tilde{C}_C(K_t, K_b, K_\alpha, K_\beta, K_\delta, K_p, K_q, K_r)\\ M_0C_m&=\tilde{C}_m=\tilde{C}_m(K_t, K_b, K_\alpha, K_\beta, K_\delta, K_p, K_q, K_r)\\ C_n&=\tilde{C}_n=\tilde{C}_n(K_t, K_b, K_\alpha, K_\beta, K_\delta, K_p, K_q, K_r)\\ M_0C_l&=\tilde{C}_l=\tilde{C}_l(K_t, K_b, K_\alpha, K_\beta, K_\delta, K_p, K_q, K_r) \end{aligned}\right\} \quad (30)$$

DETERMINATION OF REQUIREMENTS FOR DYNAMIC SIMILARITY OF RELATED BODIES IN FREE FLIGHT

The requirements for dynamic similarity of related bodies in free flight are developed on the assumption that the forces and moments on such bodies are correlated by the law of hypersonic similarity. In order to determine the conditions for dynamic similarity to be coexistent with hypersonic similarity, the dynamic equations of motion should be transformed to the same dimensionless coordinate system that was used in developing the requirements for hypersonic similarity. In addition, the velocity and force quantities should be expressed in terms of hypersonic similarity parameters.

In this dynamic system, only those forces are considered which correspond to the "power-off" conditions in free flight. The coordinate axes are taken to be principal axes of the body so that the products of inertia vanish. The dynamic equations of motion of the body are given by the relations

$$\left.\begin{aligned} u_\theta-rv+qw&=\frac{X}{\mu}\\ v_\theta-pw+ru&=\frac{Y}{\mu}\\ w_\theta-qu+pv&=\frac{Z}{\mu} \end{aligned}\right\} \quad (31)$$

$$\left.\begin{aligned} p_\theta I_{x-x}-qr(I_{y-y}-I_{z-z})&=M_x\\ q_\theta I_{y-y}-pr(I_{z-z}-I_{x-x})&=M_y\\ r_\theta I_{z-z}-pq(I_{x-x}-I_{y-y})&=M_z \end{aligned}\right\} \quad (32)$$

The translational and rotational velocities may be expressed in terms of hypersonic similarity parameters, the Mach number, and the speed of sound of the free stream by the relations

$$\left.\begin{aligned} u&=a_0M_0,\ v=-a_0K_\beta,\ w=a_0K_\alpha\\ p&=a_0\frac{K_p}{b},\ q=a_0\frac{K_q}{c},\ r=a_0\frac{K_r}{c} \end{aligned}\right\} \quad (33)$$

[2] Analogous statements can be made for the ratios of local to free-stream values of temperature, density, and Mach number.

Similarly, the aerodynamic forces and moments are given in terms of the correlation functions by the relations

$$\left.\begin{aligned} X&=\frac{\tilde{C}_D}{M_0}\left(\frac{a_0^2M_0bt\rho_0}{2}\right)\\ Y&=\tilde{C}_C\left(\frac{a_0^2M_0bt\rho_0}{2}\right)\\ Z&=\tilde{C}_L\left(\frac{a_0^2M_0bt\rho_0}{2}\right)\\ M_x&=\tilde{C}_l b\left(\frac{a_0^2M_0bt\rho_0}{2}\right)\\ M_y&=\tilde{C}_m c\left(\frac{a_0^2M_0bt\rho_0}{2}\right)\\ M_z&=\tilde{C}_n bM_0\left(\frac{a_0^2M_0bt\rho_0}{2}\right) \end{aligned}\right\} \tag{34}$$

By substituting equations (33) and (34) into equations (31) and (32), and by treating only that length of flight path over which M_0 can be considered constant, the following set of equations is obtained:

$$K_qK_\alpha+K_rK_\beta=K_\mu\tilde{C}_D \tag{35}$$

$$-\frac{dK_\beta}{d\tau}+K_r-\frac{K_pK_\alpha}{K_b}=K_\mu\tilde{C}_C \tag{36}$$

$$\frac{dK_\alpha}{d\tau}-K_q-\frac{K_pK_\beta}{K_b}=K_\mu\tilde{C}_L \tag{37}$$

$$\frac{1}{K_{x-z}K_b}\frac{dK_p}{d\tau}-\left(\frac{1}{K_{y-y}}-\frac{1}{K_{z-z}}\right)\frac{K_qK_r}{M_0^2}=\frac{K_b}{M_0^2}\tilde{C}_l \tag{38}$$

$$\frac{1}{K_{y-y}}\frac{dK_q}{d\tau}-\left(\frac{1}{K_{z-z}}-\frac{1}{K_{x-x}}\right)\frac{K_rK_p}{K_b}=\tilde{C}_m \tag{39}$$

$$\frac{1}{K_{z-z}}\frac{dK_r}{d\tau}-\left(\frac{1}{K_{x-x}}-\frac{1}{K_{y-y}}\right)\frac{K_pK_q}{K_b}=K_b\tilde{C}_n \tag{40}$$

where K_μ is given by [3]

$$K_\mu=\frac{D}{\mu} \tag{41}$$

and where

$$K_{x-x}=\frac{c^2D}{I_{x-x}} \tag{42}$$

$$K_{y-y}=\frac{c^2D}{I_{y-y}} \tag{43}$$

$$K_{z-z}=\frac{c^2D}{I_{z-z}} \tag{44}$$

$$D=\frac{cbt\rho_0}{2} \tag{45}$$

The initial conditions to this set of equations are the initial values of the hypersonic similarity parameters.

If both hypersonic similarity and dynamic similarity are to be achieved, it is required that equations (35) through (40) be independent of the Mach number as a separate variable. The elimination of M_0^2 from equation (38) is impossible in the general case, even approximately, because all the terms involved may be of comparable order of magnitude. Consequently, since equation (38) is the relation for rolling effects, it is indicated that flight paths which include rolling cannot be correlated by this method for obtaining dynamic similarity. For motions that do not involve roll, it is seen that dynamic similarity will exist for related shapes if the hypersonic similarity parameters and the dynamic similarity parameters given in equations (41) through (44) remain invariant. These dynamic similarity parameters relate the masses of the bodies and the immersing fluids, as well as the distribution of the mass in the body.

For rolling motions only, correlation can again be achieved but with a slightly different set of parameters. In this case, only equation (38) remains and can be rewritten as

$$\frac{1}{K'_{x-x}}\frac{dK_p}{d\tau}=\tilde{C}_l \tag{46}$$

where, now

$$K'_{x-x}=\frac{b^2D}{I_{x-x}} \tag{47}$$

so that correlation for pure rolling motions is now given by the hypersonic similarity parameters and the parameter K'_{x-x}.

A familiar example of motions where rolling effects would be absent is the case of motions confined to the plane of symmetry of the body, the so-called longitudinal motions. To extend the application of this law to the more general case where there are lateral motions as well as longitudinal ones, but no roll, it is necessary to have a suitable symmetry of shape and to have the inertial properties satisfy the relation

$$K_{y-y}=K_{z-z} \tag{48}$$

When these conditions are fulfilled, the flight paths of related bodies can be correlated. As an illustrative example, the disturbed motions of related missile shapes can be examined. The lengths of corresponding portions of related flight paths would be proportional to the corresponding lengths of the shapes. This property can be used to relate the amount of damping in the disturbed flight paths. As shown in Appendix B, the radii of curvature at corresponding points of the flight paths would be proportional to the product of the body length and the flight Mach number. Some of these points are illustrated in the example given in figure 3.

APPLICATION OF THE LAW TO PARTICULAR SHAPES IN STEADY FLOW

In steady flow, the three similarity parameters K_p, K_q, and K_r are zero and equations (30) reduce to the following form:

$$\left.\begin{aligned} M_0C_L&=\tilde{C}_L=\tilde{C}_L(K_t,K_b,K_\alpha,K_\beta,K_\delta)\\ M_0^2C_D&=\tilde{C}_D=\tilde{C}_D(K_t,K_b,K_\alpha,K_\beta,K_\delta)\\ M_0C_C&=\tilde{C}_C=\tilde{C}_C(K_t,K_b,K_\alpha,K_\beta,K_\delta)\\ M_0C_m&=\tilde{C}_m=\tilde{C}_m(K_t,K_b,K_\alpha,K_\beta,K_\delta)\\ C_n&=\tilde{C}_n=\tilde{C}_n(K_t,K_b,K_\alpha,K_\beta,K_\delta)\\ M_tC_l&=\tilde{C}_l=\tilde{C}_l(K_t,K_b,K_\alpha,K_\beta,K_\delta) \end{aligned}\right\} \tag{49}$$

[3] The parameter K_μ is equivalent to a familiar stability-analysis term known as the relative mass factor.

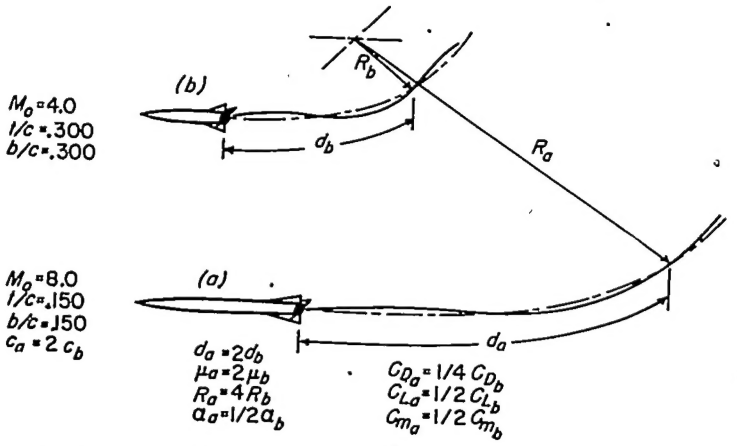

FIGURE 3.—Related wing-body combinations at hypersonic speeds.

It is important to note that the correlation of the aerodynamic coefficients given by equations (30) was obtained on the basis of two restrictions as to allowable body shapes. (See section Correlation of Aerodynamic Forces and Moments and also fig. 2). These restrictions apply equally well to equations (49).

BODIES OF REVOLUTION

For bodies of revolution, equations (49) reduce to [4]

$$\left.\begin{aligned} M_0 C_L &= \tilde{C}_L = \tilde{C}_L(K_t, K_a) \\ M_0^2 C_D &= \tilde{C}_D = \tilde{C}_D(K_t, K_a) \\ M_0 C_m &= \tilde{C}_m = \tilde{C}_m(K_t, K_a) \end{aligned}\right\} \tag{50}$$

where K_b is eliminated as it is identical to K_t.[5] It is apparent from these relations that the corresponding force and moment parameters have identical values for related bodies of revolution, provided the corresponding similarity parameters have identical values. It will now be shown that this conclusion can be generalized to include significant effects of the viscous cross forces on related inclined bodies.

The viscous cross force arises from the boundary-layer flow transverse to the body axis. A method of estimating this force along with the lift, drag, and pitching-moment coefficients associated with it has been suggested by Allen in reference 8 and is presented in Appendix C. The resulting expressions for these coefficients (see eqs. (C3) in Appendix C) are transformed to the nondimensional form, and the following relations are obtained:

$$\left.\begin{aligned} M_0 C_{L_v} &= \hat{c}_{d_c} F_1(K_t, K_a) \\ M_0^2 C_{D_v} &= \hat{c}_{d_c} F_2(K_t, K_a) \\ M_0 C_{M_v} &= \hat{c}_{d_c} F_3(K_t, K_a) \end{aligned}\right\} \tag{51}$$

For slender bodies of revolution of the type under consideration, $\hat{c}_{d_c}$ is primarily a function of the Mach number and Reynolds number of the flow component normal to the body axis. Consequently, these expressions can be reduced to the form

$$\left.\begin{aligned} M_0 C_{L_v} &= \tilde{C}_{L_v} = \tilde{C}_{L_v}(K_t, K_\alpha, R_c) \\ M_0^2 C_{D_v} &= \tilde{C}_{D_v} = \tilde{C}_{D_v}(K_t, K_\alpha, R_c) \\ M_0 C_{m_v} &= \tilde{C}_{m_v} = \tilde{C}_{m_v}(K_t, K_\alpha, R_c) \end{aligned}\right\} \tag{52}$$

where R_c is the cross Reynolds number. For small angles of attack, the cross Mach number is identical to K_α. It is clear, when comparing these relations with those of equation (50), that the latter relations apply with equal validity when viscous cross-flow effects are considered, provided that R_c is included as a similarity parameter.[6]

Nonlifting cones and ogives.—In reference 6 an analysis was performed to determine the limits of applicability of the hypersonic similarity law for nonlifting cones and ogives.[7] To determine this limit for cones, surface pressures were calculated using reference 9 and were plotted as a function of the similarity parameter K_t as shown in figure 4. A single curve favoring the slender cones was faired through the calculated points. It is apparent that the similarity in pressure holds for a wide range of values of K_t for slender cones. If it is assumed that a pressure deviation of 5 percent from the faired curve can be tolerated in using the similarity law, then limits of similarity can be determined as a function

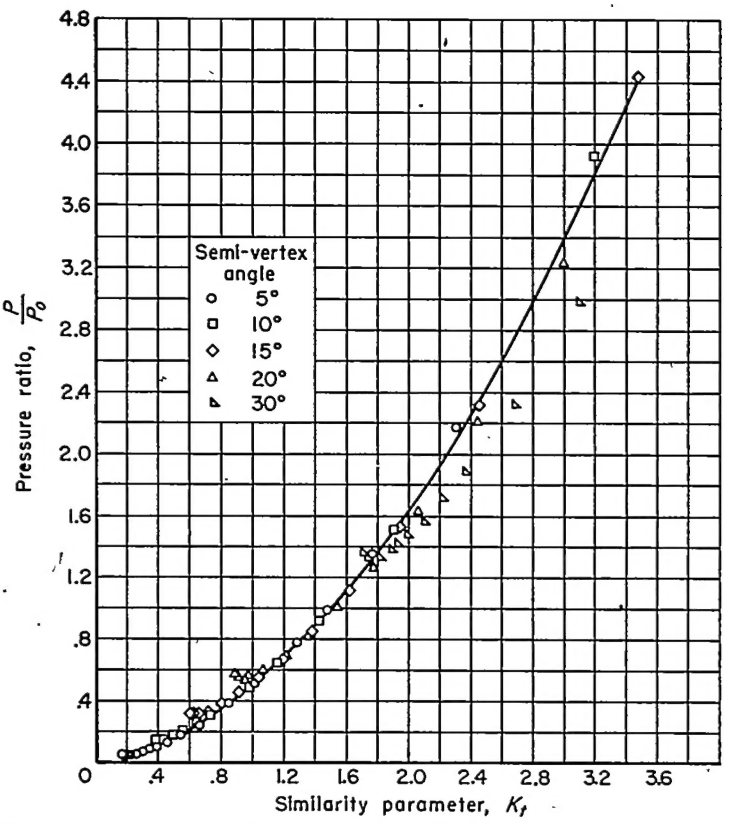

FIGURE 4.—Variation of pressure ratio, P/P_0, with similarity parameter, K_t, for nonlifting cones.

[4] Because of the axial symmetry of bodies of revolution, only angles of attack are considered. This latter consideration obviates a discussion of force and moment characteristics at angles of sideslip or combined angles of attack and sideslip, while roll, of course, has no meaning. It is clear, then, that the similarity parameters K_β and K_δ are eliminated from this analysis.

[5] If the angle of attack is zero, K_α is also zero, and the expression for the drag parameter reduces to a form equivalent to that obtained by Tsien in reference 1.

[6] It is assumed that the viscous flow considered here does not significantly influence the potential, inviscid flow discussed previously. Hence, the force and moment coefficients resulting from these flows may be superimposed.

[7] It should be noted that ogives are not exactly a related set of bodies nevertheless, they were chosen in this study since the configuration is of interest, and the deviation in thickness distribution is not significant for slender bodies.

of Mach number and fineness ratio c/t of the cone. The limits determined in this way are illustrated in figure 5 (a). The shaded area indicates the regions of Mach number and fineness ratio where the similarity law as applied to pressure on the cone will be in error 5 percent or more.

Since the surface slope of an ogive is largest at the vertex, the pressures at this point should provide a critical test for similarity of pressures. Accordingly, the limits of applicability of the law for ogives were determined in reference 6 from consideration of the pressures over a cone tangent to the ogive at the vertex. Figure 5 (b) presents the limits of applicability for ogives as obtained by this method. These results illustrate the conclusions of reference 4 that the law, as applied to nonlifting cones and ogives, is applicable over a wide range of Mach numbers and fineness ratios in spite of the simplifying assumptions made in the derivation.

A check of the applicability of the hypersonic similarity law in a rotational flow field was performed in reference 7 by comparing the pressure distributions, obtained by the method of characteristics, over ogive cylinders at several values of K_t. The pressure distributions for two ogive cylinders at a value of K_t of 2.0 are presented in figure 6 and serve to illustrate the general results obtained in reference 7. The high degree of correlation of pressures in figure 6 indicates that the hypersonic similarity law applies in a rotational flow field and verifies the analysis presented by Hayes in reference 2.

Lifting cones.—For bodies of revolution at angles of attack, a limited experimental check was made in the Ames 10-by 14-inch supersonic wind tunnel. Two cones having fineness ratios of 3.0 and 4.9 were tested at Mach numbers of 2.75 and 4.46, respectively; thus, the value of K_t was 0.91. Overlapping values of K_α up to 14° were obtained. Pressure measurements were made at the locations shown in figure 7 for angles up to 5°. The results are shown in figure 8 as a function of K_α. Agreement with the prediction of the similarity law is generally observed, in that the values of p/p_0 for corresponding points on the two bodies lie essentially along the same curve. The exception to this agreement is on the lee sides of the cones (ϵ=180°) where it is noted that significantly different curves are defined. This difference is believed to be the result of the dissimilar flow separation from the two cones, caused by the fact that identical values of R_c could not be obtained for the two cones at the same value of K_α. This difference in R_c should not affect the pressures appreciably where separation does not occur.

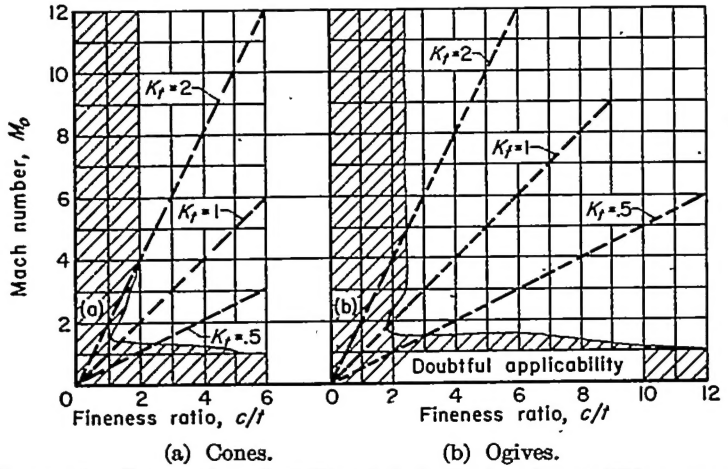

(a) Cones. (b) Ogives.

FIGURE 5.—Range of applicability of similarity law for nonlifting cones and ogives.

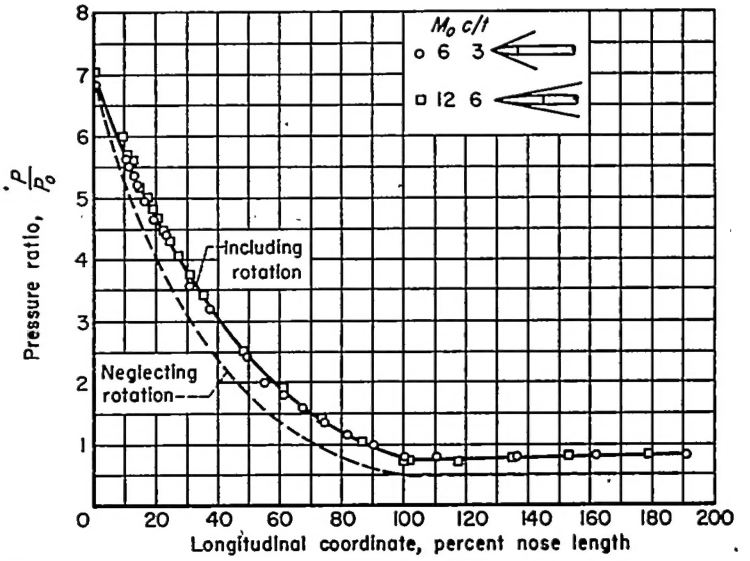

FIGURE 6.—Variation of pressure ratio, P/P_0, along nonlifting ogive cylinders for a value of the similarity parameter, K_t, of 2.0.

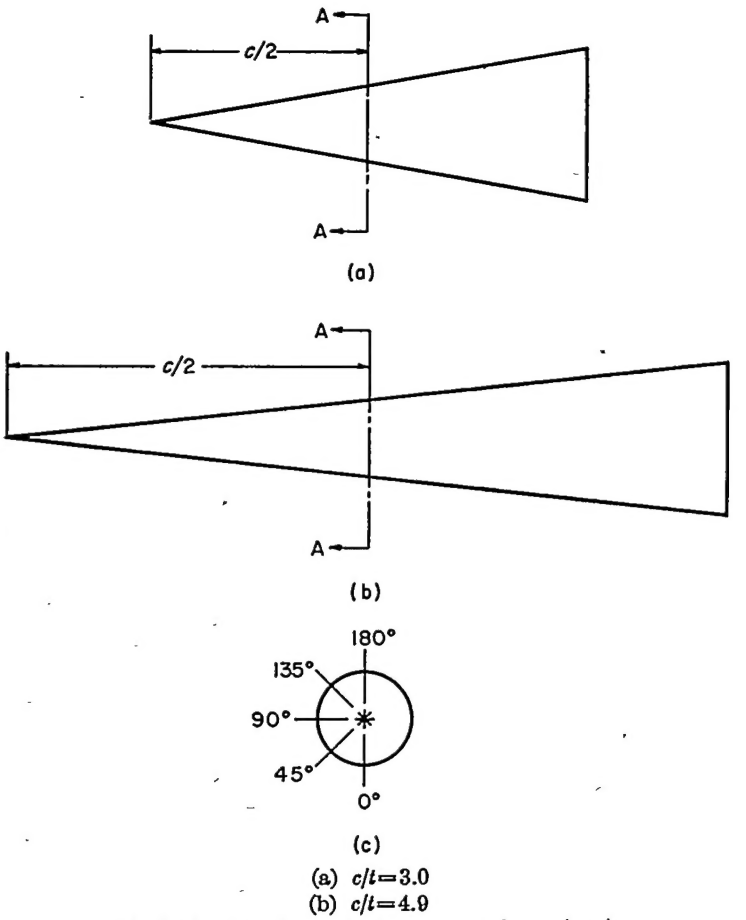

(a) c/t=3.0
(b) c/t=4.9
(c) Orifice location, ϵ, in transverse plane, A—A.

FIGURE 7.—Location of orifices on two cones tested at K_t=0.91.

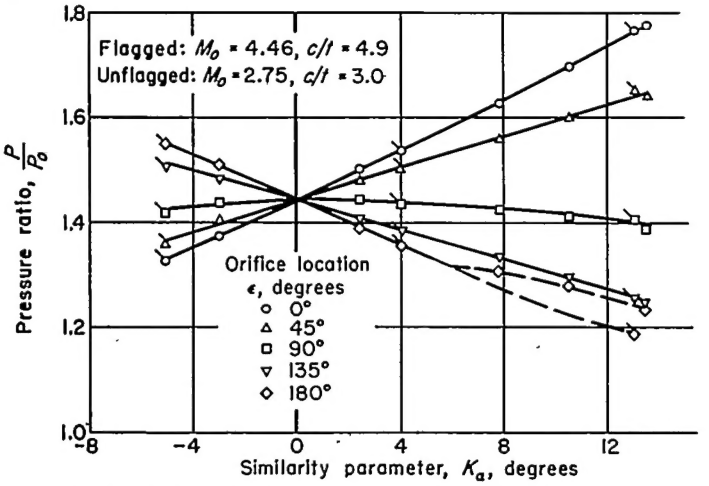

FIGURE 8.—Variation of pressure ratio, P/P_0, with K_α, for two cones tested at $K_t=0.91$.

WINGS AND WING-BODY COMBINATIONS

If, for spanwise symmetric wings, only angle of attack is considered, the similarity parameters K_β and K_δ vanish from equations (49) and only three of the aerodynamic coefficients remain. The corresponding force and moment functions are reduced to the following form: [8]

$$\left.\begin{aligned} M_0C_L&=\tilde{C}_L=\tilde{C}_L(K_t,K_b,K_\alpha)\\ M_0^2C_D&=\tilde{C}_D=\tilde{C}_D(K_t,K_b,K_\alpha)\\ M_0C_m&=\tilde{C}_m=\tilde{C}_m(K_t,K_b,K_\alpha)\end{aligned}\right\} \qquad (53)$$

These relations also apply, of course, to wing sections. In this case, b and therefore K_b are infinite and it is seen from equations (16) through (18) that the terms involving K_b vanish and the equations reduce to the two-dimensional equations for hypersonic flow. The similarity parameter K_b is thus eliminated from equation (53). This result is equivalent to that presented in reference 1.[9]

Of practical importance is the conclusion to be drawn from application of the dimensionless equation of motion (eq. (16)) and the dimensionless boundary condition (eq. (18)), to steady flow about thin wings at zero angle of yaw. It is noticed in the equations that the parameter, K_b, always appears in the form

$$\left(\frac{K_t}{K_b}\right)^2=\frac{t^2}{b^2}$$

If b is of the same order of magnitude as c, then, consistent with the other approximations made in developing this equation, the terms involving $(K_t/K_b)^2$ are to be neglected. Performing this operation, however, yields the equation of motion for two-dimensional flow. Thus, it is indicated that, if the aspect ratio is of the order of magnitude of one or greater, hypersonic flow about wings may be treated approximately as a two-dimensional-flow problem. The latter problem is, of course, relatively simple to solve.

From a physical point of view, this conclusion stems from the fact that, in supersonic flow, the effect of a disturbance at a point is confined to the conical zone formed by the Mach lines from that point. For very high Mach numbers, this zone of influence is a narrow region behind the disturbance. Consequently, conditions along a streamline are, for the most part, independent of the conditions along adjacent streamlines.[10] For thin wings in hypersonic flow, therefore, it can readily be seen that the zone of influence of disturbances caused by wing tips will, for example, be small compared to the wing area if the aspect ratio is greater than one. The effect of the tip disturbances on the aerodynamic characteristics of the wing will, of course, be correspondingly small.

Wing-body combinations may be thought of merely as irregular-shaped bodies. As such, the aerodynamic coefficients are correlated by equations (49) with the restrictions discussed in relation to these equations. The illustrative example, given in figure 3 in connection with the free-flight motion of a wing-body configuration, can be re-examined on the basis of steady flow. It is seen that in going from a Mach number of 4 to a Mach number of 8, the wing and body lengths are doubled, the angle of attack is decreased by one-half, while the body thickness and wing spans remain the same. The changes in some of the aerodynamic coefficients are also shown in the figure.

CONCLUDING REMARKS

The similarity law for nonsteady, inviscid hypersonic flow about slender three-dimensional shapes has been derived in terms of customary aerodynamic parameters. The conclusions drawn from the potential analysis used to derive the law were found to apply also to rotational flows. As a direct consequence of this law, it was found that the ratio of the local static pressure to the free-stream static pressure is the same at corresponding points in similar flow fields. With the aid of this law, expressions were obtained for correlating the forces and moments acting on related shapes in hypersonic flows.

It was found that the motions of related bodies in free flight could be correlated using the hypersonic similarity parameters and additional parameters relating the inertial properties of the bodies and the air densities. The dynamic similarity of the free flight of related bodies can be obtained for motions which include pitching and yawing but no rolling. For pure rolling motions, similarity can again be achieved.

In the case of steady flow about inclined bodies of revolution, the correlations of forces and moments derived from the similarity law can be generalized to include the significant effects of the viscous cross force.

The results of a computational analysis, using the method of characteristics, showed that the similarity law as applied to nonlifting cones and ogives is applicable over a wider range of Mach numbers and fineness ratios than might be expected from the assumptions made in the derivation.

AMES AERONAUTICAL LABORATORY,
NATIONAL ADVISORY COMMITTEE FOR AERONAUTICS,
MOFFETT FIELD, CALIF., *June 5, 1951.*

[8] Parameters equivalent to these were obtained by Tsien and, although not published, were presented in the form of lecture notes which were brought to the attention of the authors after completion of this investigation.

[9] The exponents of M_0 obtained here are different from those obtained in reference 1, because b-t is used as a reference area, rather than c-b.

[10] This result holds, in fact, for nonsteady as well as steady hypersonic flow about thin wings, as pointed out by Eggers in reference 10.

APPENDIX A

EXTENSION OF POTENTIAL FLOW ANALYSIS TO ROTATIONAL FLOW

The hypersonic similarity law can be extended to rotational flows by the method of Hayes (ref. 2). This extension is in fact demonstrated by Hayes' results. However, to understand fully the reasoning involved, it is instructive to elaborate on his analysis. Hayes showed that the hypersonic potential equation for steady flow about slender shapes was identical to the nonsteady potential equation in one less spatial coordinate under the transformation

$$x=a_0M_0\theta \tag{A1}$$

In the case of two-dimensional flow, the transformation, equation (A1), allows, for example, the upper surface of the body profile to be replaced by the upper surface of a moving piston as shown in figure 9. The piston motion must be such that a given piston displacement y_1 at time θ_1 will be the same as the ordinate on the body profile at the coordinate x_1 given by the relation $x_1=a_0M_0\theta_1$.

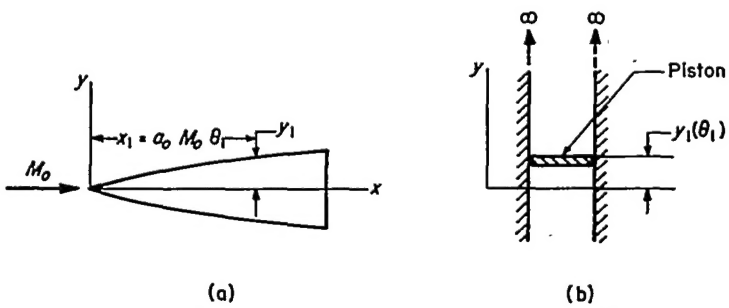

(a) Steady flow. (b) Analogous nonsteady flow.

FIGURE 9.—Two-dimensional steady flow and analogous one-dimensional nonsteady flow.

In investigating the physical significance of this transformation, Hayes pointed out that its existence resulted from the basic assumptions of slender bodies and large Mach numbers. Since, as a result of these assumptions, the x component of the fluid velocity does not change appreciably and is always much greater than the local speed of sound, there is essentially no chance for disturbances to propagate in the x direction. This is the essential feature that permits the replacement of x by the time variable θ and, hence, the existence of an analogous nonsteady flow.

Hayes further showed that in hypersonic flow about slender shapes the local Mach number remains large compared to one, even in the presence of strong shock waves caused by small surface inclinations. Consequently, the consideration of the hypersonic flow about a slender body as a nonstationary problem in one less spatial dimension remains valid when shock waves and the resultant entropy gradients are present.

One further feature of Hayes' analysis, which is not explicitly stated in reference 2, is that similarity follows directly from the existence of the analogous nonsteady flow. This feature is illustrated for two-dimensional flows as follows: The motion of the nonsteady boundary (in this case, the piston face) can be expressed in the following dimensionless form:

$$\frac{y}{t}=fn\left(\frac{a_0\theta}{t}\right) \tag{A2}$$

Upon transforming to the two-dimensional steady flow system, by the substitution of equation (A1) into the functional relationship on the right side of equation (A2), we obtain

$$\frac{y}{t}=fn\left(\frac{a_0}{t}\frac{x}{a_0M_0}\right)=fn\left(\frac{x}{c}\frac{1}{M_0\dfrac{t}{c}}\right)=fn\left(\frac{x}{c}\frac{1}{K_t}\right) \tag{A3}$$

or

$$\frac{y}{t}=fn\left(\frac{x}{c}\right),\quad K_t=\text{constant} \tag{A4}$$

Equation (A4) expresses the conditions for which the nonsteady flow system can replace a steady flow system; namely, that the body profile must be expressible in a specific nondimensional form and that the parameter, K_t, must be constant for all profiles given by this form. These are, of course, the conditions of hypersonic similitude in two-dimensional steady flow. The extension of these considerations to three-dimensional steady flow is straightforward.

To extend these concepts and results to three-dimensional, nonsteady flow, the nonsteady part of the flow may be considered, in the analogous nonsteady flow, as a nonsteady increment on the already nonsteady boundary. This can be demonstrated with reference to the potential analysis as follows: If the transformation, $x=a_0M_0\psi$, is used on the equation for steady-state hypersonic flow in perturbation form [11]

$$M_0^2\varphi_{xx}-\left[1-(\gamma-1)\frac{M_0}{a_0}\varphi_x-\frac{\gamma+1}{2}\frac{\varphi_y^2}{a_0^2}-\frac{\gamma-1}{2}\frac{\varphi_z^2}{a_0^2}\right]\varphi_{yy}-$$
$$\left[1-(\gamma-1)\frac{M_0}{a_0}\varphi_x-\frac{\gamma-1}{2}\frac{\varphi_y^2}{a_0^2}-\frac{\gamma+1}{2}\frac{\varphi_z^2}{a_0^2}\right]\varphi_{zz}+2\left(\frac{M_0}{a_0}\varphi_y\varphi_{xy}+\right.$$
$$\left.\frac{\varphi_y\varphi_z\varphi_{yz}}{a_0^2}+\frac{M_0}{a_0}\varphi_z\varphi_{xz}\right)=0 \tag{A5}$$

there is obtained the equation

$$\frac{\varphi_\psi\varphi_\psi}{a_0^2}-\left[1-(\gamma-1)\frac{\varphi_\psi}{a_0^2}-\frac{\gamma+1}{2}\frac{\varphi_y^2}{a_0^2}-\frac{\gamma-1}{2}\frac{\varphi_z^2}{a_0^2}\right]\varphi_{yy}-$$
$$\left[1-(\gamma-1)\frac{\varphi_\psi}{a_0^2}-\frac{\gamma-1}{2}\frac{\varphi_y^2}{a_0^2}-\frac{\gamma+1}{2}\frac{\varphi_z^2}{a_0^2}\right]\varphi_{zz}+$$
$$2\left(\frac{\varphi_y\varphi_{\psi y}}{a_0^2}+\frac{\varphi_y\varphi_z\varphi_{yz}}{a_0^2}+\frac{\varphi_z\varphi_{\psi z}}{a_0^2}\right)=0 \tag{A6}$$

By applying the same transformation to the nonsteady flow equation

[11] In all the equations of this section, the wind axes are made to coincide with the body axes in order not to obscure the argument.

$$\varphi_{\theta\theta}+M_0^2\varphi_{xx}-\left[1-(\gamma-1)\frac{M_0}{a_0}\varphi_x-\frac{\gamma+1}{2}\frac{\varphi_y^2}{a_0^2}-\frac{\gamma-1}{2}\frac{\varphi_z^2}{a_0^2}-(\gamma-1)\frac{\varphi_\theta}{a_0^2}\right]\varphi_{yy}-\left[1-(\gamma-1)\frac{M_0}{a_0}\varphi_x-\frac{\gamma-1}{2}\frac{\varphi_y^2}{a_0^2}-\frac{\gamma+1}{2}\frac{\varphi_z^2}{a_0^2}-(\gamma-1)\frac{\varphi_\theta}{a_0^2}\right]\varphi_{zz}+2\left(\frac{M_0}{a_0}\varphi_y\varphi_{xy}+\frac{M_0}{a_0}\varphi_z\varphi_{xz}+\frac{\varphi_y\varphi_z}{a_0^2}\varphi_{yz}\right)+2\left(\frac{M_0}{a_0}\varphi_{x\theta}+\frac{\varphi_y}{a_0^2}\varphi_{y\theta}+\frac{\varphi_z}{a_0^2}\varphi_{z\theta}\right)=0 \tag{A7}$$

with an additional variable change of

$$\Omega=\theta+\psi \tag{A8}$$

the same equation (A6) is obtained with ψ replaced by Ω. Hence, Hayes' conclusions concerning steady-state, three-dimensional flow should apply equally well to nonsteady, three-dimensional flows.

APPENDIX B

CORRELATION OF THE FLIGHT-PATH CURVATURE

Consider related bodies moving through properly related fluids in paths of finite radii of curvature. Equating the centrifugal force to the side force, the following relation is obtained:

$$\mu\frac{V_0^2}{R}=C_C\frac{1}{2}\rho_0V_0^2A \tag{B1}$$

After rearranging in terms of similarity parameters, equation (B1) becomes

$$\frac{M_0c}{R}=\tilde{C}_CK_\mu\frac{A}{bt}=\text{constant} \tag{B2}$$

The parameter M_0c/R correlates the radii of curvature at corresponding points of similar flight paths.

This conclusion is also true for curved flight in the vertical plane.

APPENDIX C

FORCES AND MOMENTS DUE TO VISCOUS CROSSFLOWS ON BODIES OF REVOLUTION

In reference 11, Prandtl demonstrated that laminar viscous flows over infinitely long inclined cylinders may be treated by considering, independently, the components of the flow normal and parallel to the axis of the cylinder. Jones, in reference 12, applied this concept to the study of boundary-layer flows over yawed cylinders. The work of Prandtl and Jones suggests, as indicated by Allen in reference 8, that the cross force on slender inclined bodies of revolution may be estimated in the following manner: Each cross section of the body is treated as an element of an infinite cylinder of the same radius. The cross force per unit length on such a cylinder is given by the following equation:

$$s_p=rc_{d_c}\rho_0V_0^2\sin^2\alpha \tag{C1}$$

The incremental lift, drag, and moment produced by this cross force are then given by the relations

$$\left.\begin{aligned}\text{lift}&=rc_{d_c}\rho_0V_0^2\sin^2\alpha\cos\alpha\\ \text{drag}&=rc_{d_c}\rho_0V_0^2\sin^3\alpha\\ \text{moment}&=rxc_{d_c}\rho_0V_0^2\sin^2\alpha\end{aligned}\right\} \tag{C2}$$

Retaining leading terms in α and integrating over the body, where $r=r(x)$, the aerodynamic coefficients are given by the equations

$$\left.\begin{aligned}C_{L_v}&=\frac{2\hat{c}_{d_c}\alpha^2}{A}\int_0^\circ r\,dx\\ C_{D_v}&=\frac{2\hat{c}_{d_c}\alpha^3}{A}\int_0^\circ r\,dx\\ C_{m_v}&=\frac{2\hat{c}_{d_c}\alpha^2}{Ac}\int_0^\circ rx\,dx\end{aligned}\right\} \tag{C3}$$

where the reference area is proportional to the maximum cross-sectional area of the body, and the reference length is the body length. The coefficient $\hat{c}_{d_c}$ is the mean c_{d_c} for the body of revolution, and has therefore been taken outside the integral.

REFERENCES

1. Tsien, Hsue-shen: Similarity Laws of Hypersonic Flows. Jour Math. and Phys., vol. 25, no. 3, Oct. 1946, pp. 247–251.
2. Hayes, Wallace D.: On Hypersonic Similitude. Quart. Appl. Math, vol. V, no. 1, Apr. 1947, pp. 105–106.
3. Oswatitsch, Klaus: Similarity Laws for Hypersonic Flow. KTH Aero TN 16, Royal Inst. of Tech., Division of Aeronautics, Stockholm, Sweden, 1950.
4. Goldsworthy, F. A.: Two-Dimensional Rotational Flow at High Mach Number Past Thin Aerofoils. Quart. Jour. Mech. and Appl. Math., vol. V, pt. 1, Mar. 1952, pp. 54–63.
5. Lin, C. C., Reissner, Eric, and Tsien, H. S.: On Two-Dimensional Non-Steady Motion of a Slender Body in a Compressible Fluid. Jour. Math. and Phys., vol. 27, no. 3, Oct. 1948, pp. 220–231.
6. Ehret, Dorris M., Rossow, Vernon J., and Stevens, Victor I.: An Analysis of the Applicability of the Hypersonic Similarity Law to the Study of Flow About Bodies of Revolution at Zero Angle of Attack. NACA TN 2250, 1950.
7. Rossow, Vernon J.: Applicability of the Hypersonic Similarity Rule to Pressure Distributions Which Include the Effects of Rotation for Bodies of Revolution at Zero Angle of Attack. NACA TN 2399, 1951.
8. Allen, H. Julian: Pressure Distribution and Some Effects of Viscosity on Slender Inclined Bodies of Revolution. NACA TN 2044, 1950.
9. Mass. Inst. of Tech., Dept. of Elec. Engr., Center of Analysis: Tables of Supersonic Flow Around Cones, by the Staff of the Computing Section, Center of Analysis, under the direction of Zdenek Kopal. Tech. Rep. No. 1, Cambridge, 1947.
10. Eggers, A. J., Jr.: On the Calculation of Flow About Objects Traveling at High Supersonic Speeds. NACA TN 2811, 1952.
11. Prandtl, L.: On Boundary Layers in Three-Dimensional Flow. Ministry of Aircraft Production, Volkenrode VG 84. (Reports and Translations No. 64) May 1, 1946.
12. Jones, R. T.: Effects of Sweep-back on Boundary Layer and Separation. NACA Rep. 884, 1947.